Fourth International Meeting on Wind Turbine Noise

Rome Italy 12-14 April 2011

Coherence Issues in Wind Turbine Noise Assessment

Bruce E. Walker
Channel Islands Acoustics
676 W Highland Dr
Camarillo, CA 93010 USA
bwalker@channelislandsacoustics.com

Abstract

Conventional modelling of sound propagation between arrays of wind turbines and the surrounding environment treats the individual turbines as compact sources combining various components, including blade trailing-edge radiation, blade tip radiation, mechanical equipment sources, inflow turbulence/blade interaction, blade/tower interaction, etc. The A-weighted, C-weighted, 1/3-Octave or Octave Band acoustic power (actually mean-square sound pressure) from each turbine is computed at individual or a grid of off-site positions and summed over all turbines in the array to determine off-site impact of the array. This process includes the tacit assumption that the acoustic signals from the turbines are statistically independent. In actuality, measurements of turbine installations spanning over 25 years show clear departures from this assumption, particularly as regards mechanical and low frequency blade-induced sound components. Since these components tend to be important factors in indoor annoyance from wind turbine noise, it is desired to avoid underestimating them.

Statistical analyses and audio demonstrations will be presented to illustrate the effect of quasi-random coherence on subjective tonality for small and large arrays of turbines. Graphical analyses of measurement data will be presented to illustrate the effect of chance synchronizations on the amplitude of low frequency pulsations.

The effect of signal coherence among multiple mechanical sources operating at similar speeds on the measured and subjective tonality of individual turbines will be discussed and demonstrated.

Introduction

A consistent theme encountered in over 25 years of consulting on wind turbine related noise issues has been “you should have been out here last ____ when it was *really* noisy.” Despite sound level readings in the 45 dB range, residents have used terminology such “deafening,” “sounds like a freight train coming over the hill” and the like to describe their post-turbine acoustical environments at regulatory body meetings. It is well known that atmospheric conditions can significantly affect the propagation of sound over the source to receiver distances commonly encountered in wind turbine installations, but occasional enhanced prominence of distinctively

"wind turbine" sounds may arise from the coherent nature of these distinct sounds rather than as a result of propagation modulation.

Nomenclature

L, LZ, SPL	Sound Pressure Level in decibels (dB)
LA, SLA	L with A-weighting
L_{eqT}	Level of mean-square sound pressure, period *T*
L_{maxT}	Maximum Sound Pressure Level, period *T*
lg	Logarithm to base 10
$<>_T$	Time Average over Period *T*
p	Sound Pressure (usually in pascals (Pa))
R	Correlation Coefficient
AC	Dimensional Auto Correlation (usually Pa^2)
CC	Dimensional Cross Correlation (usually Pa^2)
P_{ref}	Reference Sound Pressure 20 μPa
t	Dimensional Time (seconds)
τ	Correlation Function Delay (seconds)
f	Dimensional Frequency (Hz)
ϕ	Phase Angle (radians)

Background

Equation (8) of IEC standard 61400-11

$$L_s = 10\lg\left[10^{(0{,}1L_{s+n})} - 10^{(0{,}1L_n)}\right] \tag{1}$$

provides a convenient way to correct turbine noise measurements for background noise, based on the presumption that for a multiple source situation, the total sound pressure level is determined by simply adding the squared sound pressures from all sources and computing 10 lg of the result:

$$L_{total} = 10\lg\left[\sum_{i=1,N} 10^{(0{,}1L_i)}\right] \tag{2}$$

or

$$L_{total} = 10\lg\left[\sum_{i=1,N} \left\langle \frac{p_i(t)^2}{p_{ref}^{\ 2}} \right\rangle_T\right] \tag{3}$$

where $<>_T$ denotes time average over period T.

This formulation is the basis of most multi-source prediction models and most tables and nomographs for "adding decibels." However, it is only correct for sources that satisfy important specifications.

The principal of superposition requires that in a linear medium, the sound pressure at any point and time that results from multiple sources is equal to the sum of the pressures.

$$p_{total}(t) = \sum_{i=1,N} p_i(t) \tag{4}$$

which suggests that for the total sound field

$$L_{total} = 10\lg\left[\left\langle\left(\sum_{i=1,N}\frac{p_i(t)}{p_{ref}}\right)^2\right\rangle_T\right] \tag{5}$$

or

$$L_{total} = 10\lg\left[\sum_{i=1,N}\left\langle\frac{p_i(t)^2}{p_{ref}^{\ 2}}\right\rangle_T + \sum_{i\neq j}\left\langle\frac{p_i(t)p_j(t)}{p_{ref}^{\ 2}}\right\rangle_T\right] \tag{6}$$

In order for Eq. (6) and Eq. (3) to give the same answer, the N^2-N cross-products on the right side of (6) must average out to zero over time period T, which appears to be a tall order. However, for most broadband noise generation processes, each of these cross-products averages to zero individually within modest time intervals (i.e. they are statistically independent).

The important exceptions are periodic signal components, for which there is no guarantee of a zero average. Dispensing with p_{ref} (=20 μPa) and recognizing p is actually time dependent and a ratio to p_{ref}, each cross-product term is

$$\left\langle p_i p_j\right\rangle_T = \left(\left\langle p_i^{\ 2}\right\rangle_T\left\langle p_j^{\ 2}\right\rangle_T\right)^{0,5} R_{ij,T} \tag{7}$$

where $R_{ij,T}$ is the correlation coefficient $1 \geq R \geq -1$. For signals with periodic components of equal or very similar frequencies, Eq. (3) assumes the distribution of cross-products is sufficiently random that the average of the terms is near zero. The potential consequences of this assumption are the topic of this paper.

Correlation Function and Unaligned Coherence

Often when measuring in “hostile” environments, important periodic signal components can be buried in background noise. An extension of the correlation coefficient concept shown in Eq. (7) and its frequency domain counterpart may be used to reveal the buried information.

The correlation function is the delay-dependent cross product of a signal with itself (autocorrelation function) or between two signals (cross correlation function)

$$\begin{aligned} AC_{i,i}(\tau)_T &= \left\langle p_i(t)p_i(t-\tau)\right\rangle_T \\ CC_{i,j}(\tau)_T &= \left\langle p_i(t)p_j(t-\tau)\right\rangle_T \end{aligned} \tag{8}$$

$AC(0)$ is the mean-square value of the signal (and the Fourier transform of $AC(\tau)$ is the power spectral density).

For partially coherent pairs of signals, $CC(\tau)$ exhibits a peak value for τ equal to the delay time between sensors.

For stochastic signals AC and CC decrease rapidly from the peak.

For sinusoidal signals, regardless of phase, $AC(\tau)$ is always $\cos(2\pi f\tau)$. Cross-correlation properties for tonal signals are summarize in (9) below:

$$\begin{aligned} p(t) &= P\sin(2\pi ft + \phi) \\ \left\langle p_i(t)p_j(t-\tau)\right\rangle_{T\to\infty, f_i = f_j} &= \cos(2\pi f\tau + \phi_2 - \phi_1) \\ \left\langle p_i(t)p_j(t)\right\rangle_{T\to\infty, f_i \neq f_j} &= 0 \\ \left\langle p_i(t)p_j(t)\right\rangle_{T, f_i \neq f_j} &= \text{[See Figure 1]} \end{aligned} \tag{9}$$

Figure 1 below shows the effect of averaging time of the cross-correlation between two tones of similar but unequal frequency and initial phase. The horizontal axis is non-dimensional T x $(f_2 - f_1)$. For example, to have insignificant effect on a measurement with averaging time 10 seconds, the frequency difference would need to be greater than approximately 0.4 Hz.

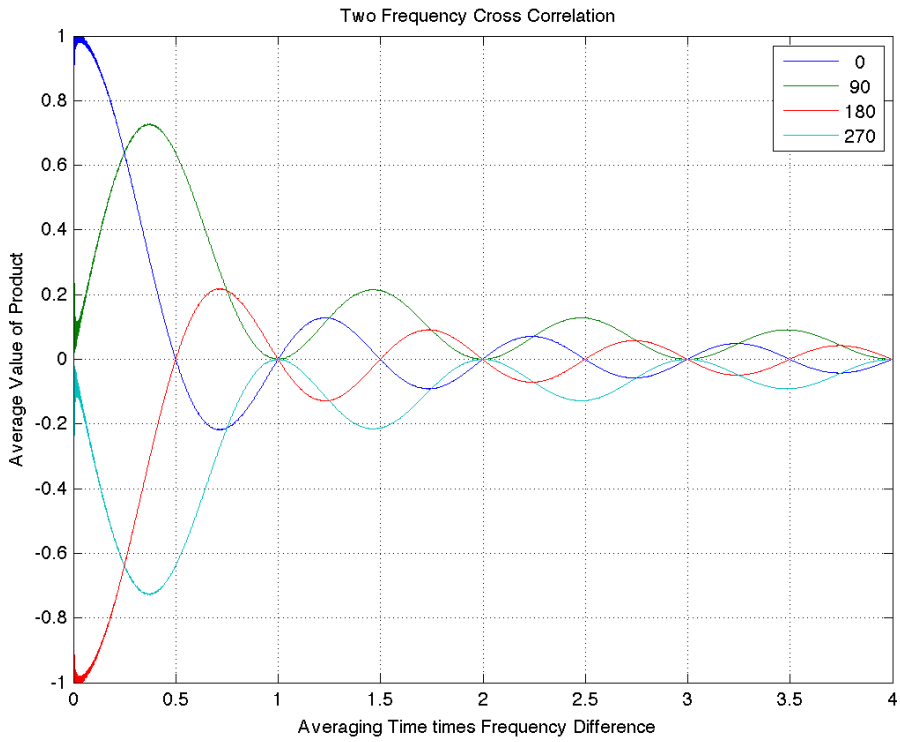

Figure 1. Illustration of cross correlation between two tones of near equal frequency as function of non-dimensional averaging time $T\Delta F$ and initial phase offset (degrees)

The sequence of figures to follow demonstrates the power of correlation analysis to reveal potentially problematic periodic components buried in background noise.

Figure 1 shows low frequency noise 94 dB (blue), once per second pulses with peak level 104 dB (green) and the summation signal (red). Although the pulses can be seen in the composite signal, it is not clear that they would be identified without a-priori knowledge.

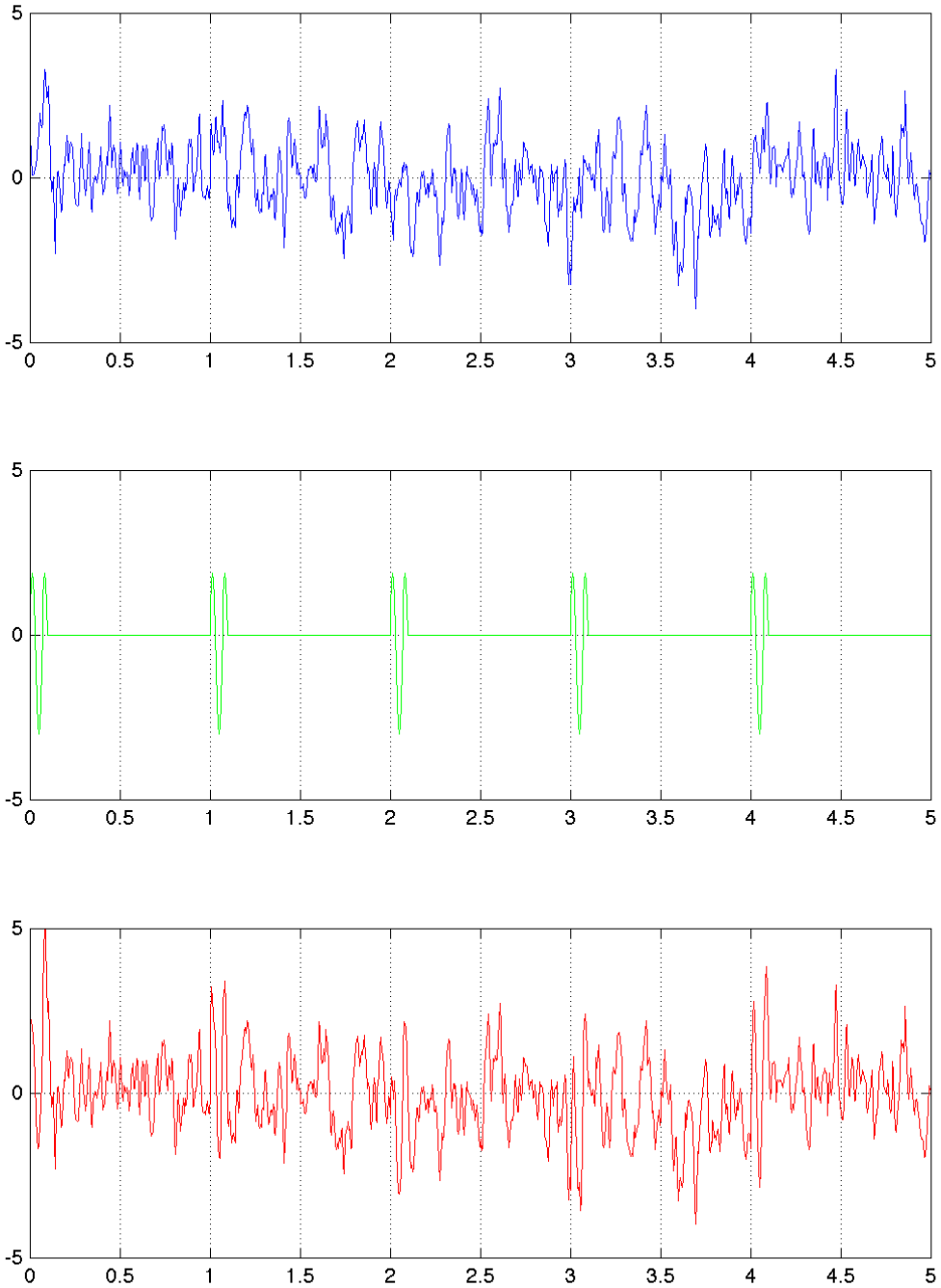

Figure 2. Low Frequency Noise, Synthesized Wake Pulses, Composite Waveforms

Figure 3 shows the 1 Hz bandwidth frequency spectra for the three signals. Although the effect of the pulses is evident in the 10-20 Hz range of the composite (red) spectrum, it provides no indication of the repetitive impulsive character of the signal.

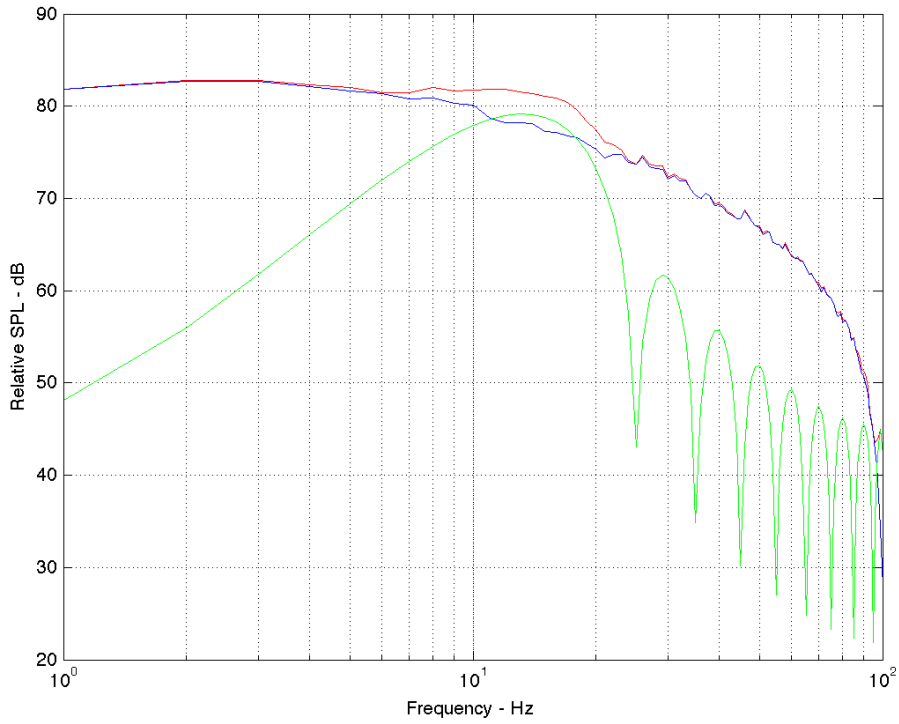

Figure 3. Spectra Corresponding to the Time Histories in Figure 1

The autocorrelation functions (for the delay range -1.5 to +1.5 seconds) for this signal sequence is shown in Figure 3.

Note that the autocorrelation at zero delay is 1 for the noise, equalling the mean-square value of the signal.

Note that the autocorrelation of the pulses is 0.3, approximately 10 dB below the noise, while the peak amplitude of the pulse was 3.0, 10 dB above the average level of the noise. The one second repetition rate and the relatively narrow pulse width are clearly indicated (although the peak amplitude of the pulses can only be estimated).

Finally note that since the noise and pulses are not correlated with each other, the autocorrelation of the composite at zero delay is 1.3, the sum of the autocorrelations for the noise and pulses separately.

For purposes of wind turbine low frequency noise measurements, it is generally possible to greatly improve signal to noise ratios by using two measurement systems spaced a few meters apart and compute $CC(\tau)$. The difference between wind speed, ground turbulence and sound speed then affords a means to separate acoustic noise from a measurement object from spurious noises. This is shown in Figure 4 and Figure 5 below.

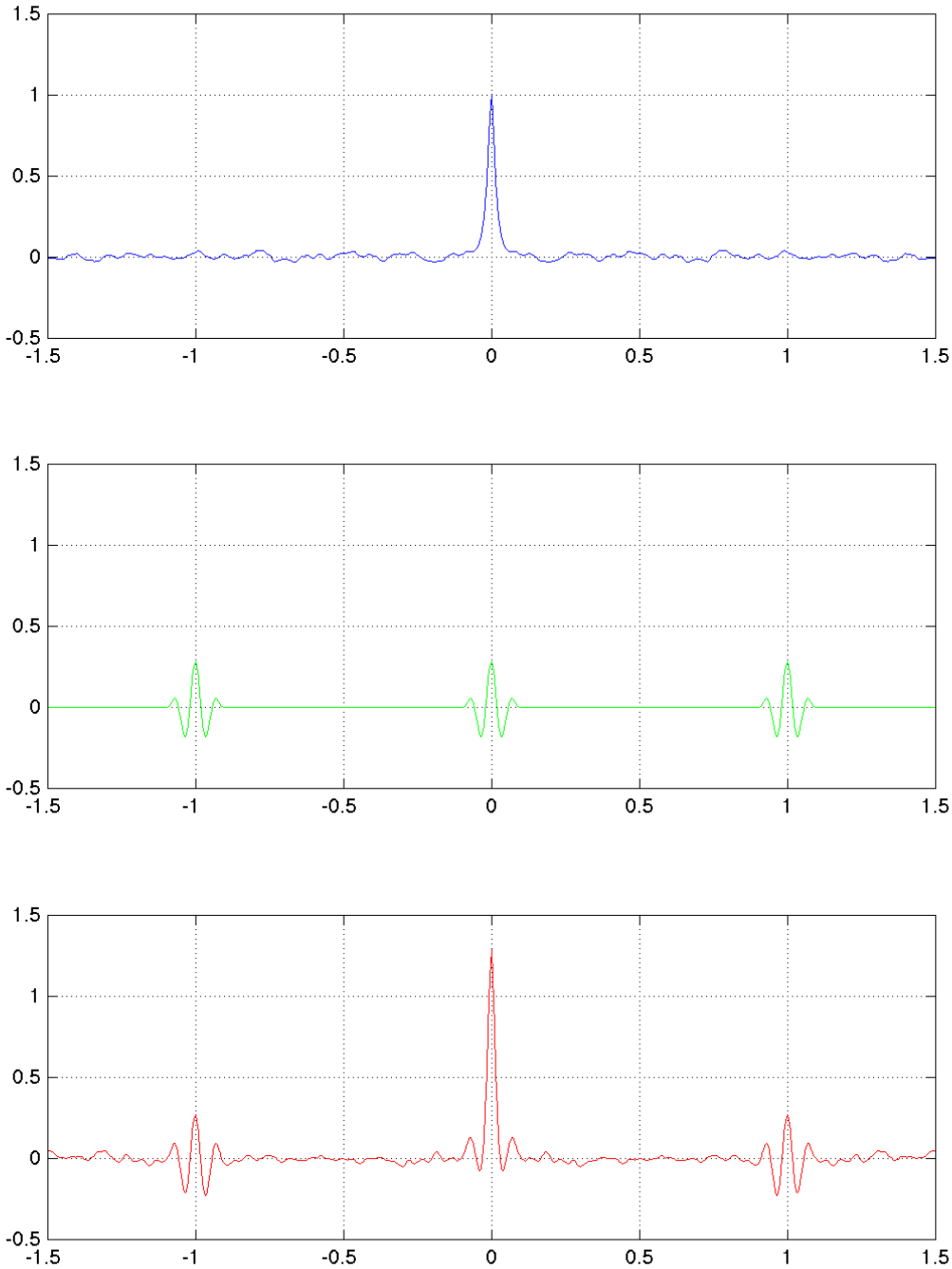

Figure 4. Autocorrelation Functions for Signals in Figure 1 (Blue = Random Noise, Green = Pulse Sequence, Red = Composite)

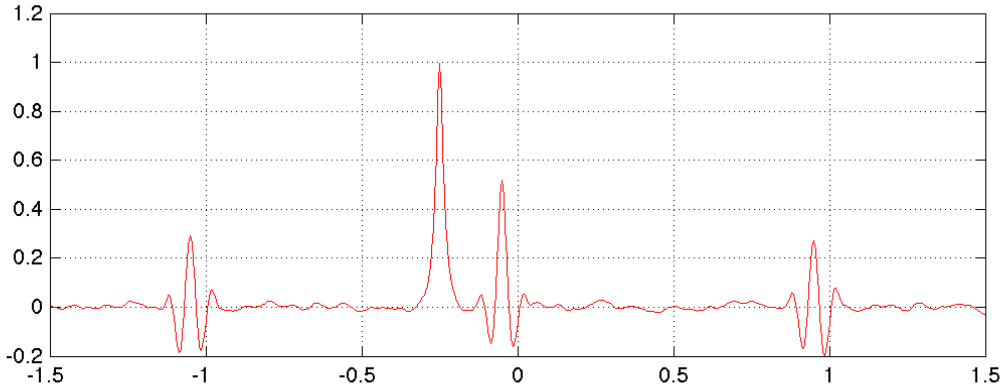

Figure 5. Hypothetical separation of combined measurement object broadband and pulse noise from slowly propagating turbulence noise using cross correlation of signals from two microphones spaced 35 meters “downwind

Geoffrey Miles of NASA/Glenn Research Center has developed a frequency domain corollary concept dubbed Unaligned Coherence to identify tones in turbofan combustor environment.

Wind Turbine Noise Components

The major contributions to wind turbine noise had been established and well documented by the early 80's thanks to work by Hubbard and Shepherd, Sutherland et al at Wyle Labs, Kelley at NREL, and many others. Details of some of the sources have been revealed by recent phased array and focused sensor studies by Oerlemans and others. The following listing is for reference and not intended as revelatory or all-inclusive:

1. Inflow turbulence – rotor blade interaction. Predominantly low to mid-low frequency broadband noise with very low to no correlation between pairs of turbines in "typical" installations.
2. Blade turbulent boundary layer – trailing edge radiation. Predominantly mid to mid-high frequency broadband noise with no correlation between pairs of turbines.
3. Mechanical vibrations and acoustic radiation from turbine power train. Tones typically in the 100-1000 Hz range excited by gear meshing and generator magnetostriction or periodic deformation. High correlation between excited radiating surfaces and fluctuating correlation between pairs of turbines operating at near-equal speeds.
4. Mechanical vibrations and acoustic radiation from auxiliary equipment. Combination of broadband noise and tones in the 100-1000 Hz range from cooling fans, pumps, transformers, yaw drive. High correlation of tone components between elements on individual turbines and between pairs of turbines.
5. Support tower – blade interaction. Pulsations at blade passage rate (0,5 – 10 Hz) as blades pass through flow deficit of support tower. Most prominent with rotor downwind of tower. High correlation between turbines in similar flow environments.
6. Blade wake – support tower interaction. Pulsations at blade passage rate (0,5 – 10 Hz) as blade wakes impinge support tower. Most prominent with rotor upwind of tower. High correlation between turbines in similar flow environments.
7. Rotor – flow profile interaction. Low frequency radiation from rotor blades due to periodic loading in shear flow or with rotor yaw error.

The sources above that may be identified in the field as "wind turbine noise" are largely in the "coherent" category, suggesting it would be prudent to consider effects of partially coherent summations in turbine noise modelling.

To illustrate, representative measured noise spectra for two relatively modern large wind-turbines are shown in Figure 6.

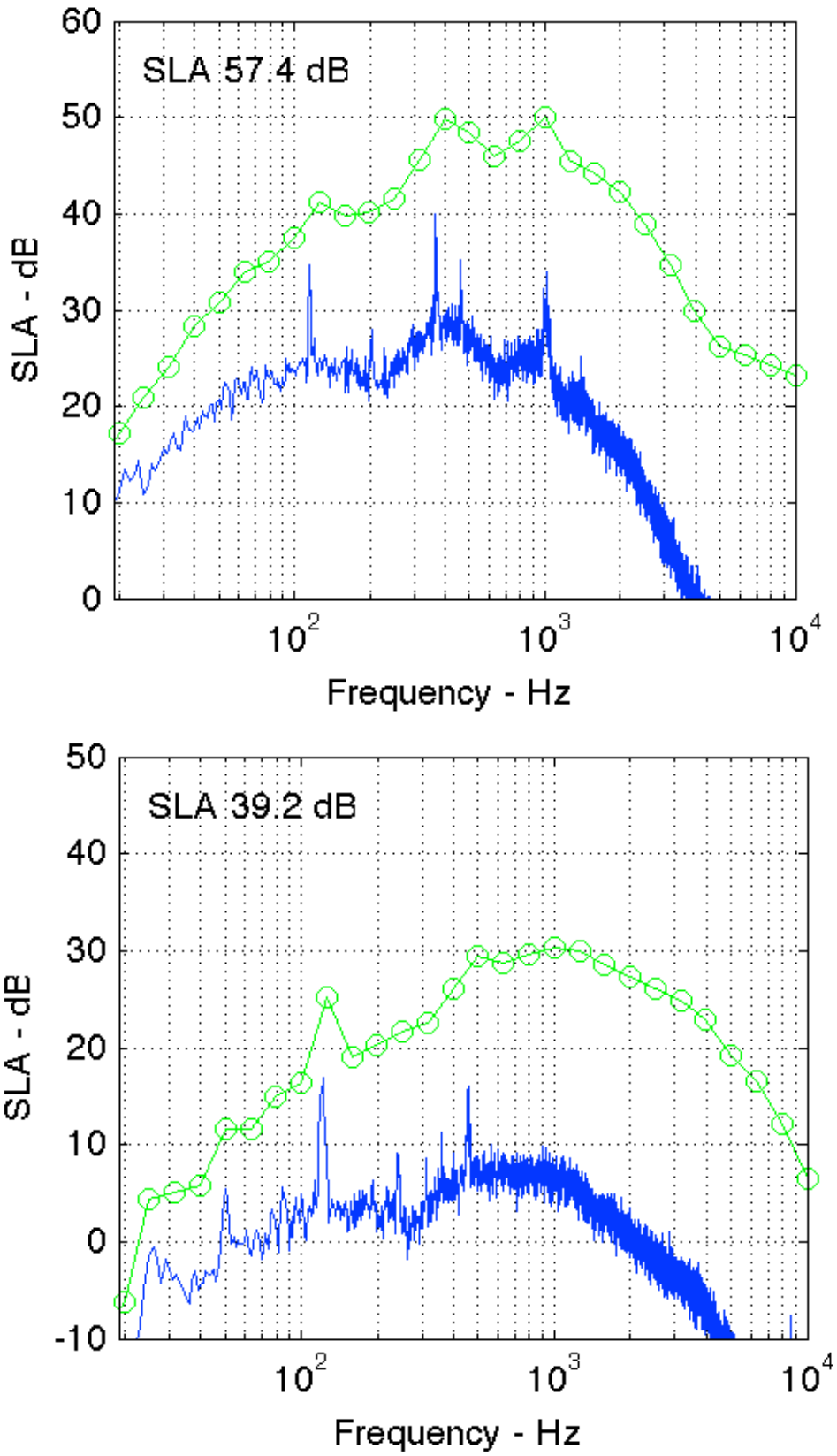

Figure 6 - Representative Wind Turbine Noise Spectra – $L_{eq10sec}$

In each case the green curve is the 1/3-octave and the blue curve is nominal 1-Hz spectral levels. It is clear that both spectra exhibit various tonal components, but none would invoke a "tone penalty" under most noise exposure standards in the U.S.

An example of periodic low frequency pulsations from a modern turbine are shown in Figure 7 as cross correlations computed from microphones 670 and 700 meters upwind of the turbine. It corresponds with the lower graph in Figure 5.

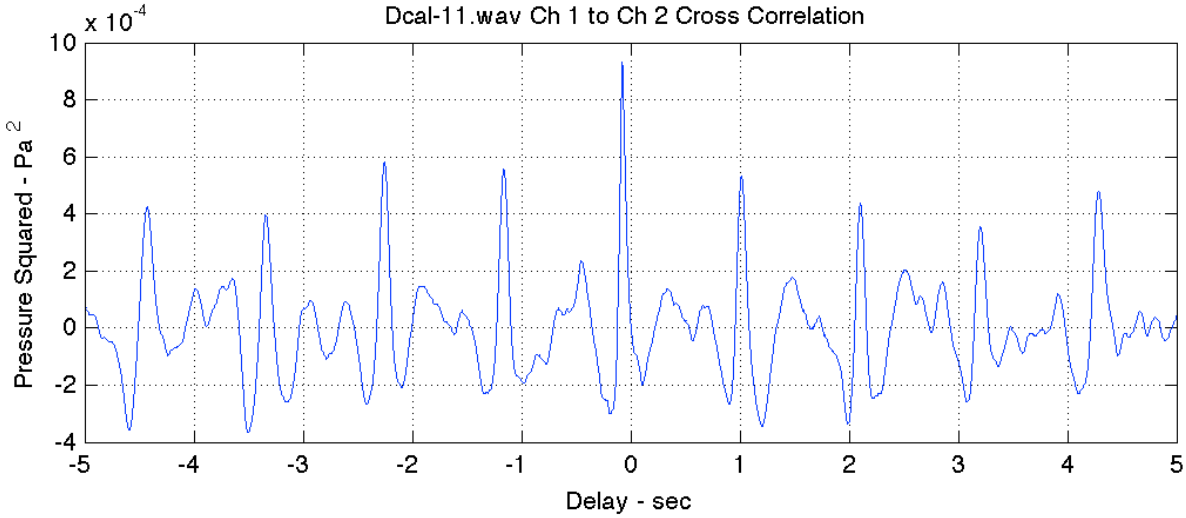

Figure 7. Example of Low Frequency Periodic Wind Turbine Noise

Relevant observations from this chart are:

1. The peak cross correlation occurs at a delay of about 80 ms, in agreement with the 30 m microphone spacing.
2. The peak correlation corresponds to LZ 63.8 dB, significantly higher than the LA 39.2 dB shown in Figure 1 and suggestive of a predominance of low frequency noise Note that the peak autocorrelation (not shown) is LZ 71.8 dB at both microphones, illustrating the power of using cross correlation to assess low frequency noise in windy environments).
3. There is a repetitive component of period approximately 1.1 seconds, suggesting that the three-blade turbine is turning at just over 18 RPM.
4. The pulse width of the periodic component is about 0.1 second and the signal level is equivalent to LZ 62 dB

The autocorrelation of the noise from Figure 7, measured *inside* a residence about 720 meters from the turbine is shown in Figure 8. Overall noise level is LZ 61.4 dB and LA approximately 22 dB. The periodic "thump" level is LZ 57.2 dB.

In both Figure 7 and Figure 8, the peak amplitude of the "thump" can only be estimated from the correlations. Based on the apparent duty cycles, the peak amplitude is on the order 10 dB greater than the overall LZ, i.e. 72 dB outdoors and 67 dB indoors.

These are not excessive sound levels. However, we will demonstrate that the coherent nature of the tones in Figure 6 and the "thumps" in Figure 7 can result in their protruding above the background more than the overall noise in turbine arrays.

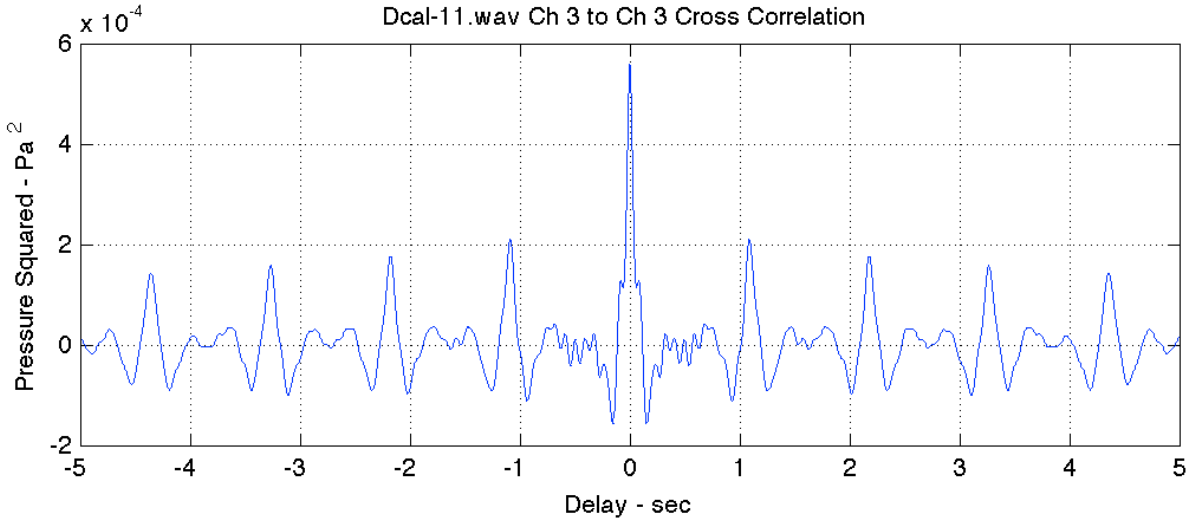

Figure 8. Example of Low Frequency Noise Measured Indoors

Turbine Simulation

In order to demonstrate the potential effect of signal coherence on noise from moderate size arrays of turbines, several scenarios were synthesized.

1. Multiple turbines emitting a tone of fixed frequency but arbitrary phase. This would represent, for example, turbines with cooling fans emitting pronounced blade-passage tones, typically in the 150-300 Hz range
2. Multiple turbines emitting tones of slightly different frequency, representative of gear-meshing in a variable-speed turbine.
3. Multiple turbines emitting rotor blade passage rate thumps.

Synthesized signals from the total array were added together and characterized by maximum sound pressure level, time-average (L_{eq}) sound pressure level and level fluctuation. Phase combinations were assessed using Monte Carlo approach for large arrays and by direct evaluation for smaller arrays (observe that for phase increment of 3 degrees, a five-turbine array would have over $2x10^8$ combinations to evaluate).

For the tone cases, a nominal frequency of 150 Hz was chosen arbitrarily. For the thumps, waveforms similar to that shown in Figure 2 were used, with a 1 Hz blade passage rate (20 RPM).

Simulation Results

Fixed-Frequency Tones

Figure 9 shows the not-unexpected result for two turbines. When the phases align, the level is 3 dB greater than for two uncorrelated sources and when the phases are 180°, the signals cancel. The dividing point is 90° and therefore the level is greater than uncorrelated 50% of the time.

Three turbines, as shown in Figure 10, begin to show a different trend. The maximum is 10 lg(5) or just below +5 dB but the probability of exceeding the uncorrelated SPL is only about 40%. Figure 11 and Figure 12 show that an “assmptotic” trend develops, with probability of worst-case becoming miniscule.

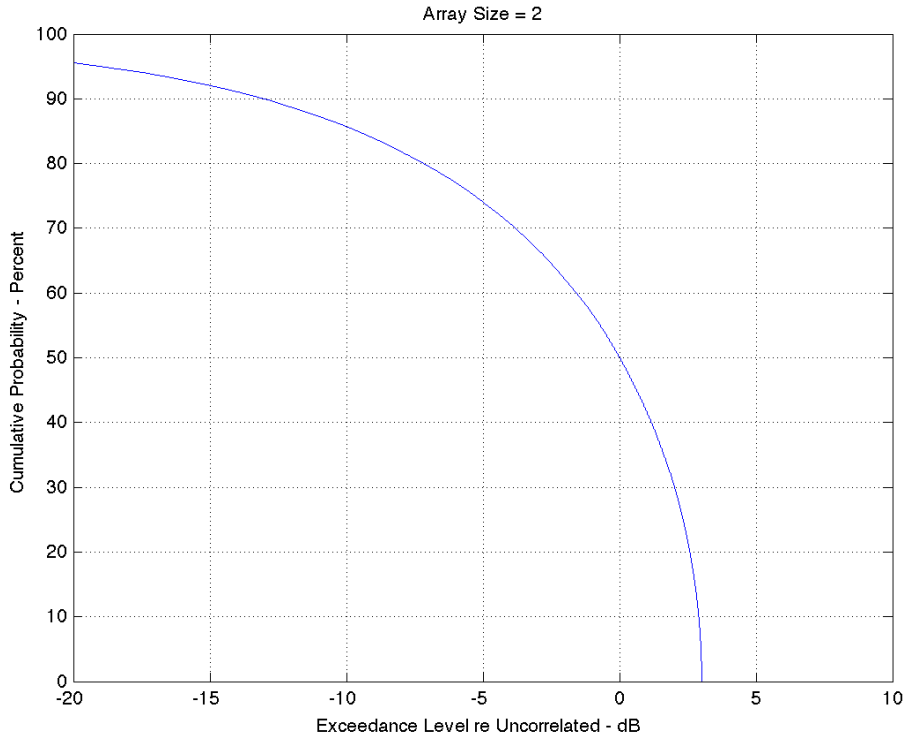

Figure 9. Relative SPL probability for 2 turbines at 150 Hz, all possible phases

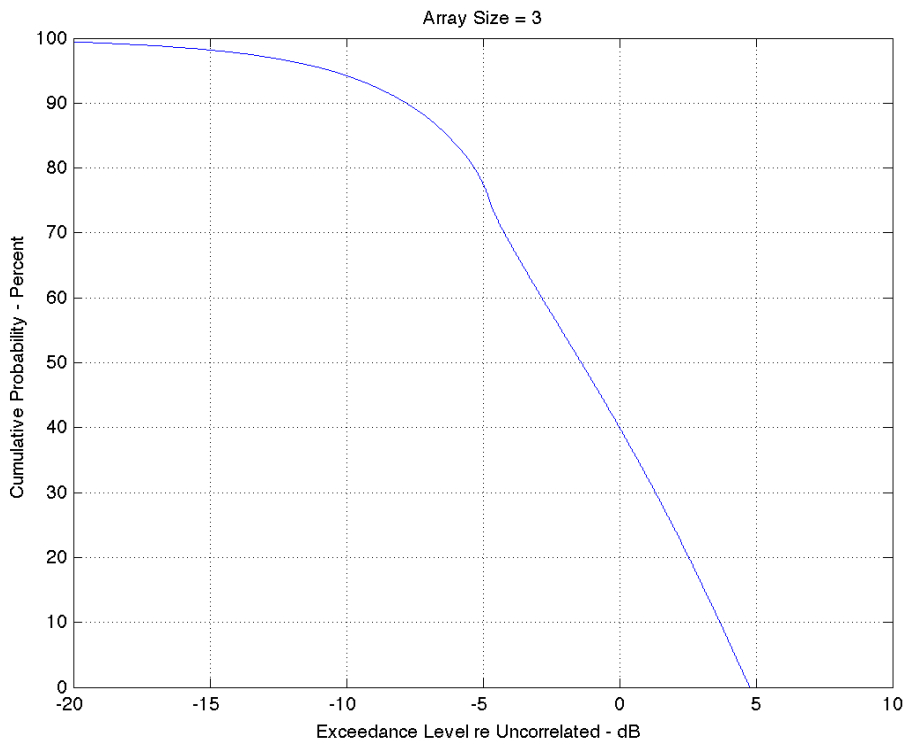

Figure 10. Relative SPL probability for 3 turbines at 150 Hz, all possible phases

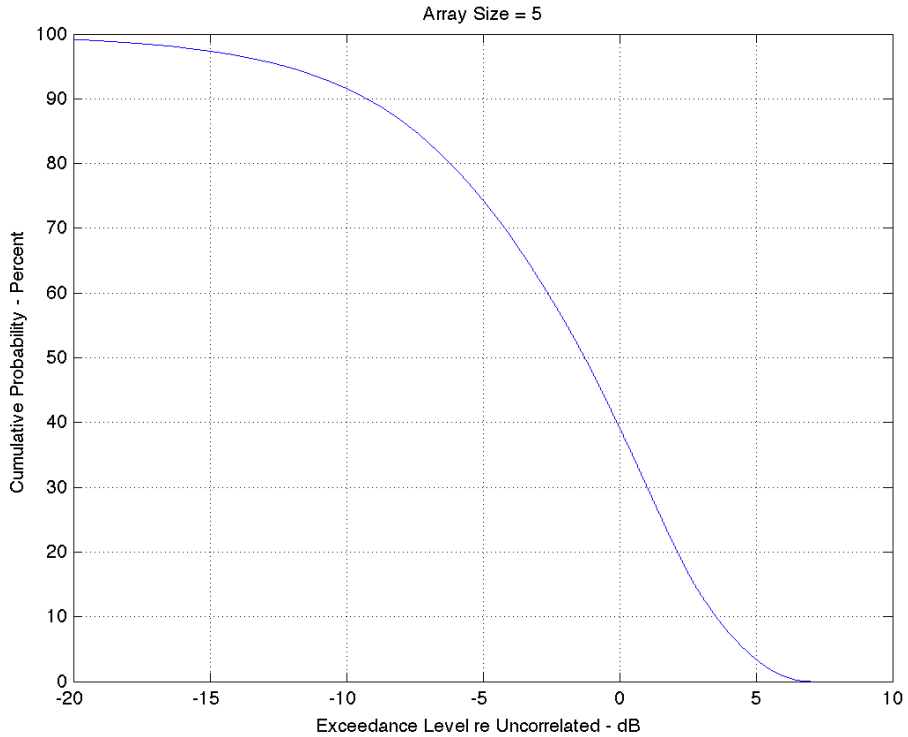

Figure 11. Relative SPL probability for 5 turbines at 150 Hz, all possible phases

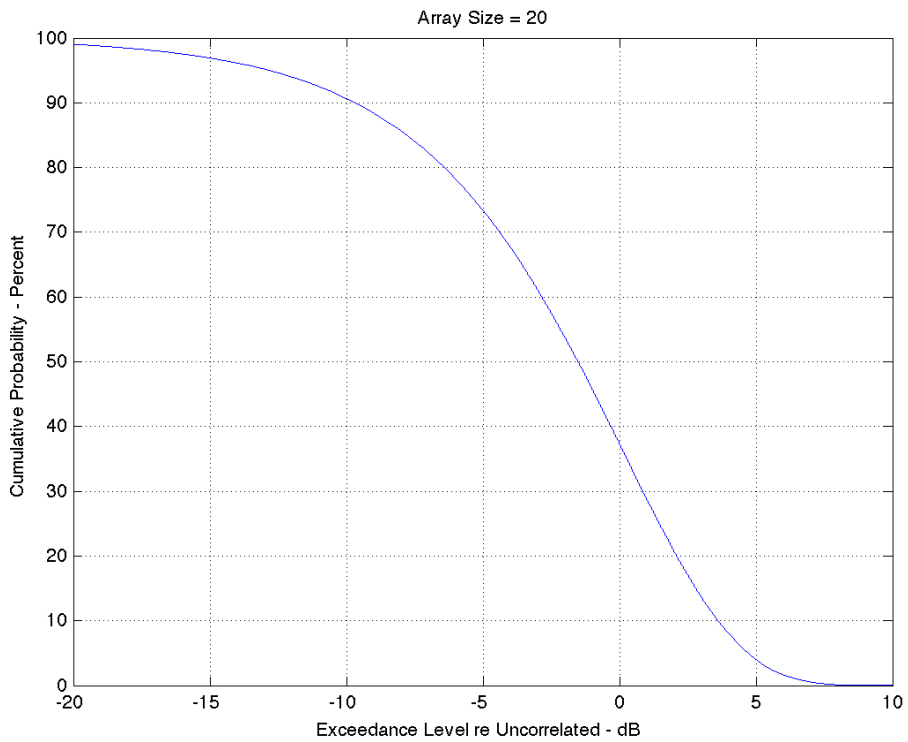

Figure 12. Relative SPL probability for 20 turbines, 6×10^6 point Monte Carlo phase combinations (truncated at -20 to +10 dB)

The distributions shown in the prior four figures suggest that for fixed-frequency tones, the probability of exceeding the uncorrelated tone level by over 3 dB is about 10% and the probability of exceeding it by 5 dB is 2-3%.

They also suggest that if the phases among the turbines are constantly changing (such is if the frequencies are slightly different), considerable amplitude modulation might be expected. One example of this is shown in the following set of graphs.

Distributed Frequency Tones

First, Figure 13 shows a randomly selected distribution of tone frequencies 150 ± 2.5 Hz for a relatively large (20) source array. The initial phases of these signals were randomized and the signals added together for a one-hour period and a running one-second block- L_{eq1sec} was saved. The $L_{eq1hour}$ was also computed.

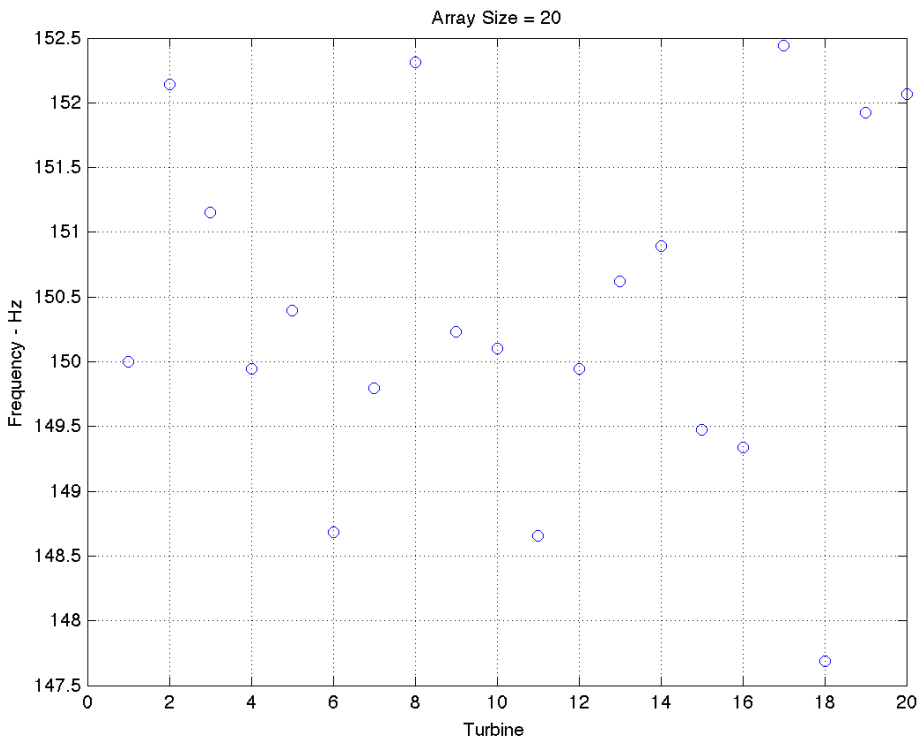

Figure 13. Hypothetical 20 Turbine tone frequency distribution

The first minute of the time history of L_{eq1sec} for this distribution are plotted relative to the uncorrelated sum of the signals in Figure 14. Also shown in green is the value of $L_{eq1hour}$, which is within 0.01 dB of the uncorrelated value. Note that protrusions 3-6 dB above the uncorrelated level are not uncommon. The distribution for the full hour computation is shown in Figure 15. The one-second averaging time has resulting in a compression of the fixed-frequency, random phase case shown in Figure 12. Logarithmic plot Figure 16 illustrates the effect of time averaging on the maximum composite signal level, which is limited to +7 dB from the +13 dB possible (though extremely improbable) for the fixed frequency case.

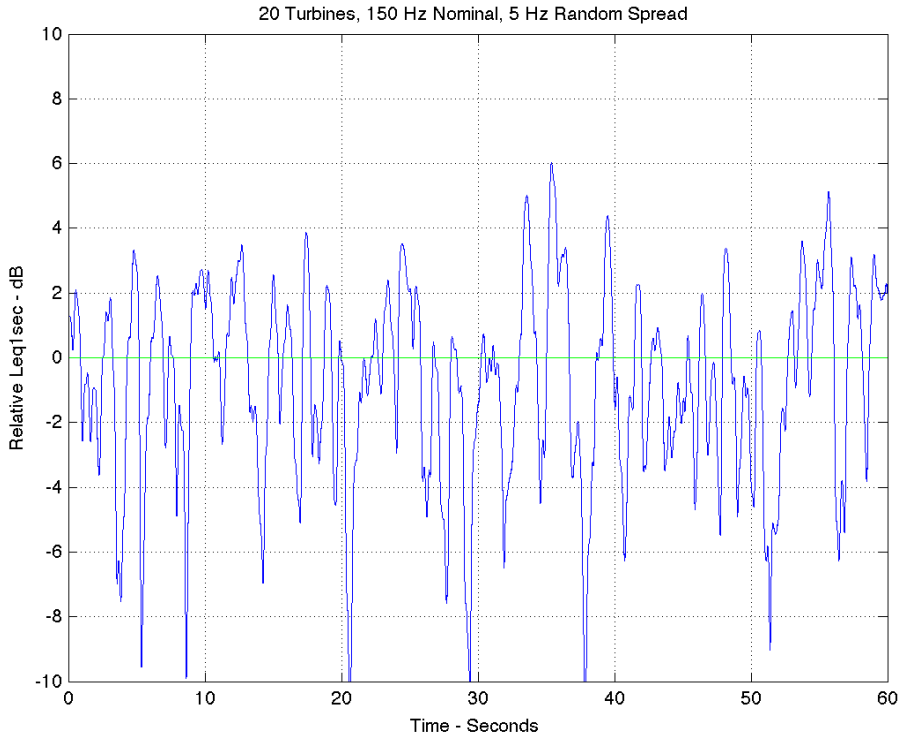

Figure 14. One-minute example of L_{eq1sec} (blue) and $L_{eq1hour}$ (green) of the frequency distribution shown in Figure 13

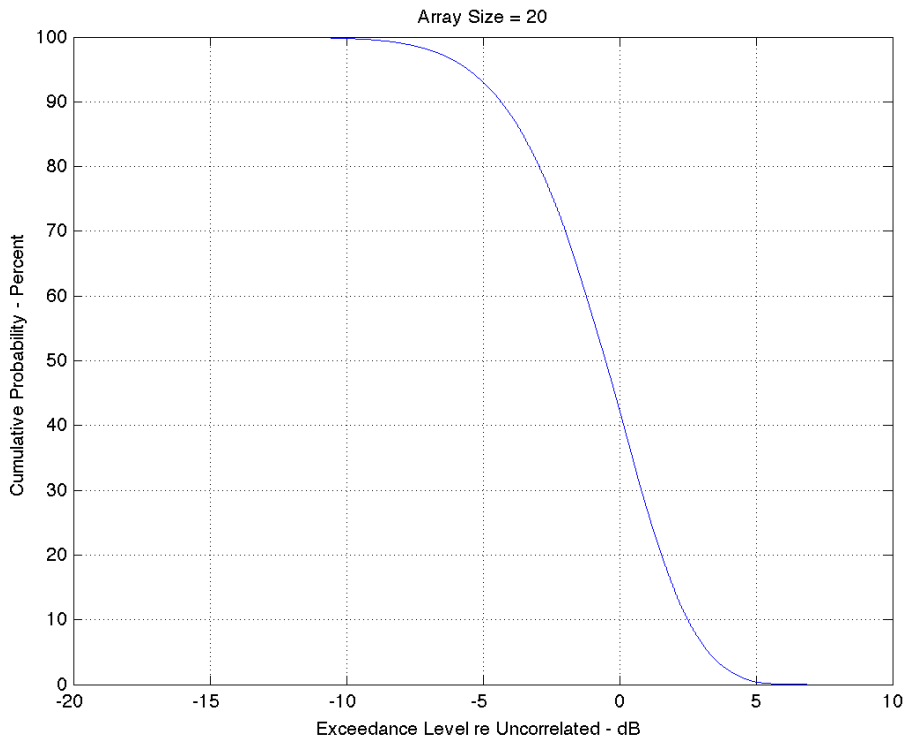

Figure 15. Statistical distribution for one hour of 20 frequency-distributed sources

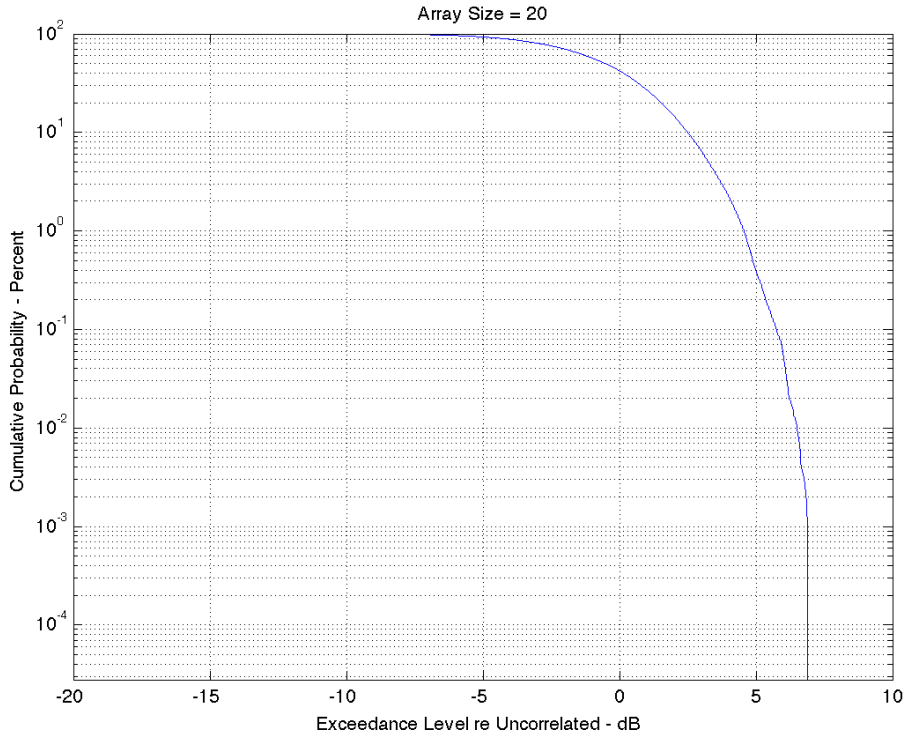

Figure 16. Logarithmic representation of Figure 15

Rotor Blade Thumps

Statistical distributions for low frequency pulsation noise are distinct from tones because of their low duty cycle. i.e. during periods of non-overlap, they would add incoherently. The effect of the low frequency pulsations is largely the result of the peak or maximum sound pressure rather then the average value as with tones and broadband noise because interaction with non-linear processes such as window rattle tend to be the primary subjective manifestation

To illustrate the contrast between tones and thumps statistics, Figure 17 and Figure 18 may be compared with Figure 9 and Figure 10, respectively. In this case the pulse waveform simulation shown in Figure 2 was used/

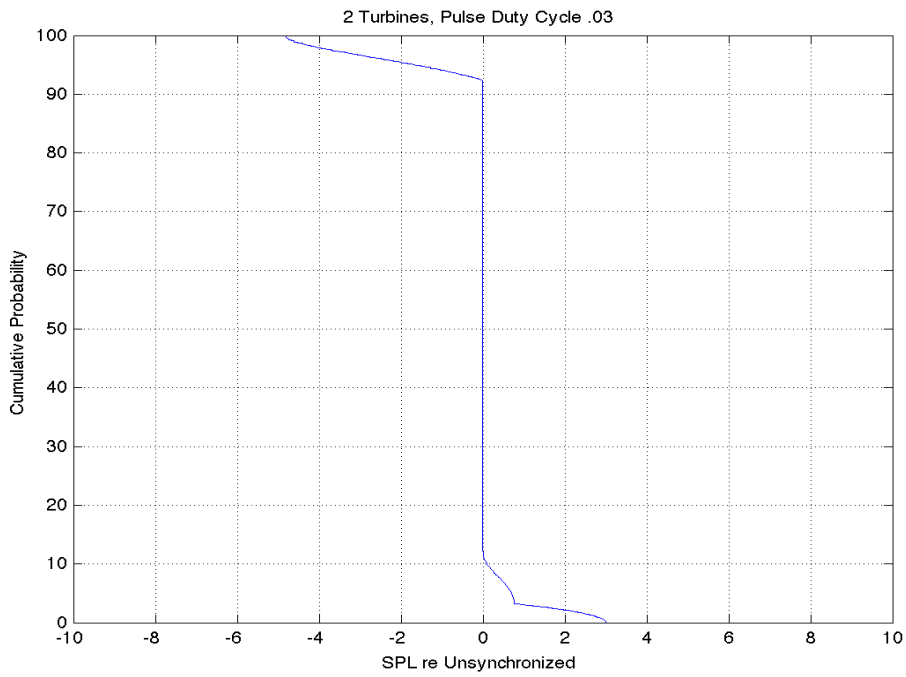

Figure 17. Statistics of average Thump SPL for 2 turbines

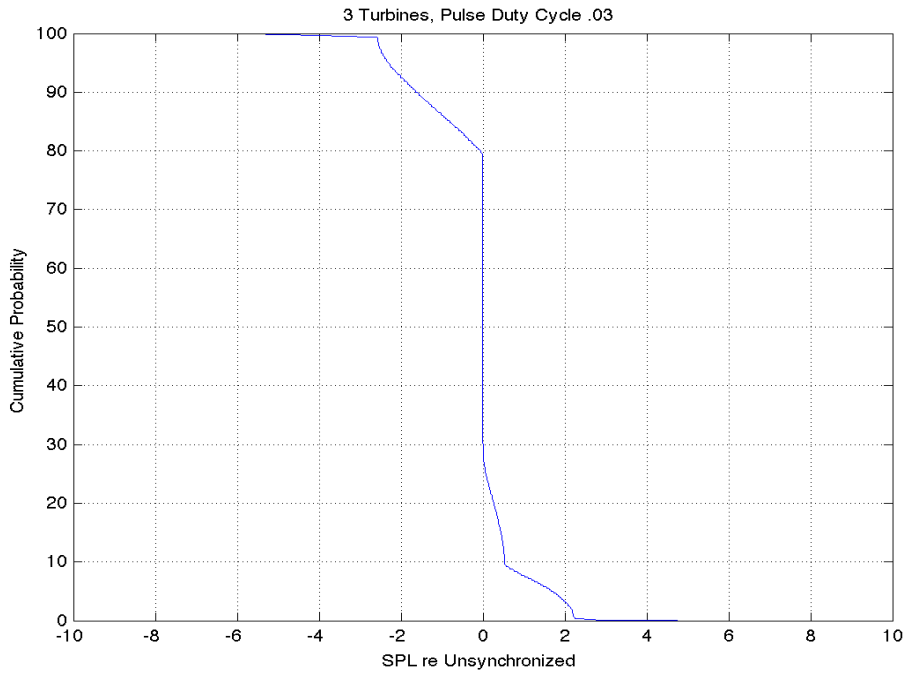

Figure 18. Statistics of average Thump SPL for 3 turbines

To model arrays of more than three turbines, a pulse simulation was prepared with a sharper primary pulse and more spread pre- and post-cursor pulses as shown in Figure 19. Several random, best and worst-case alignments of these pulse models were synthesized, with results as shown in histogram and cumulative distribution plots, Figure 20 and Figure 21.

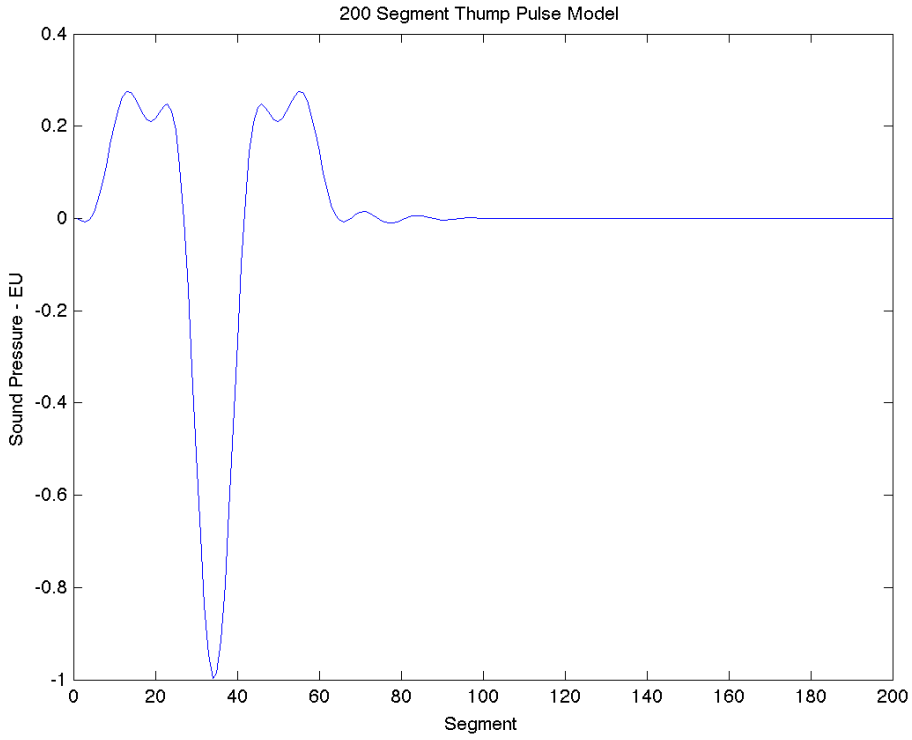

Figure 19. Pulse model used for 5-turbine thump simulations

In the histogram, maximum and average levels were accumulated in 0.2 dB bins for a total of 30^4 orientation combinations. With a maximum sound pressure of 1 Pa, single turbine sound pressure levels were computed at 80.5 dB L_{eq} and 94 dB L_{max}, illustrated by the green and red lines on the graph. The blue line is the uncorrelated SPL for 5 turbines, 87.5 dB. It is clear that for L_{eq} (blue) the mode is near the uncorrelated sum. For L_{max} (red) the mode is the single turbine maximum. Maximum levels 14 dB above the mode and average levels 7 dB above the mode are possible, but with miniscule probability. The cumulative distributions illustrate that a 10 dB or greater rise in L_{max} has just under 1% probability of occurring.

A six-hour simulation of five turbines turning at a random distribution of speeds ±1% around 20 RPM is shown in Figure 22 though Figure 25. At the six-hour scale, intrusions above the uncorrelated prediction appear brief, albeit frequent. However the expanded views show that the excess noise events might last for a substantial fraction of a minute. This could be disconcerting to a resident whose windows were just below the rattle threshold most of the time.

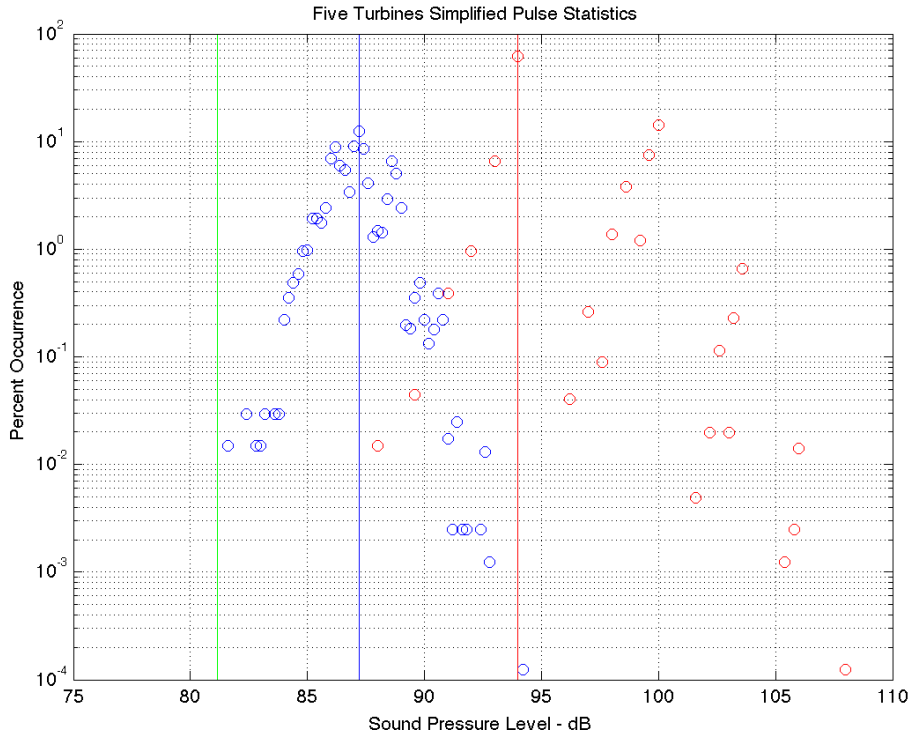

Figure 20. SPL Histogram for combinations of all spacings of pulses from 5 turbines in 4 degree rotor orientation increments

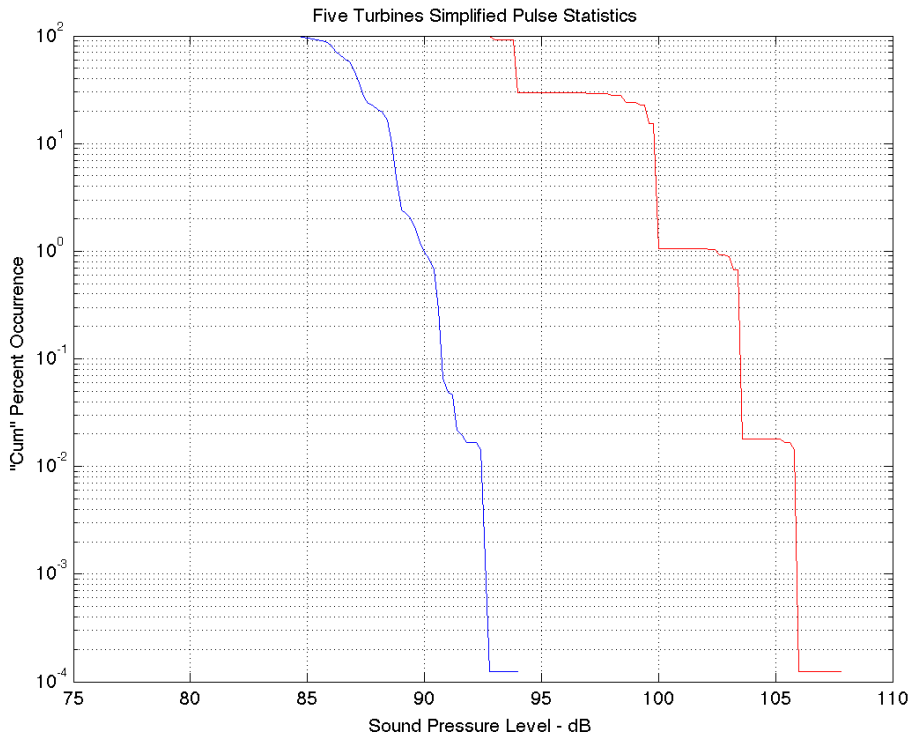

Figure 21. SPL Distribution for combinations of spacings of pulses from 5 turbines

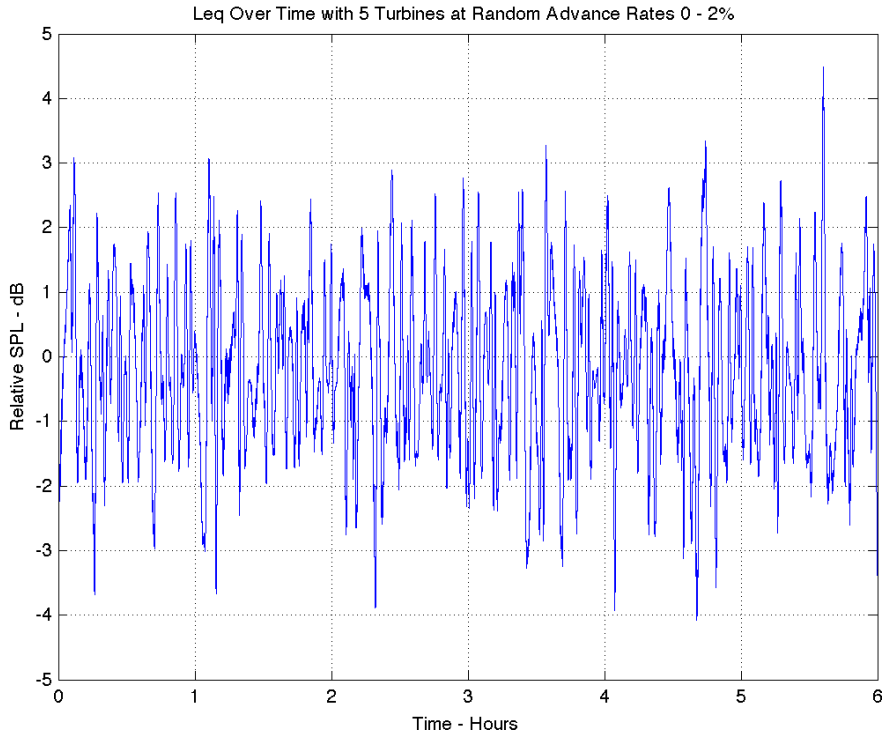

Figure 22. Six hour thump simulation with 5 turbines - L_{eq1sec} re uncorrelated sum

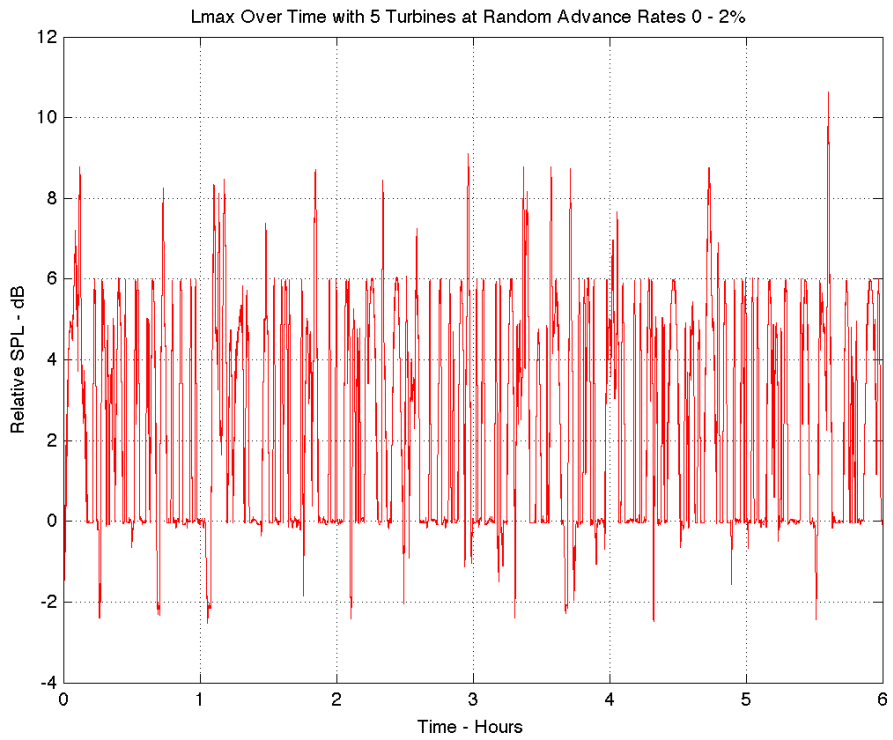

Figure 23. Six hour thump simulation with 5 turbines – $L_{max1sec}$ re single turbine

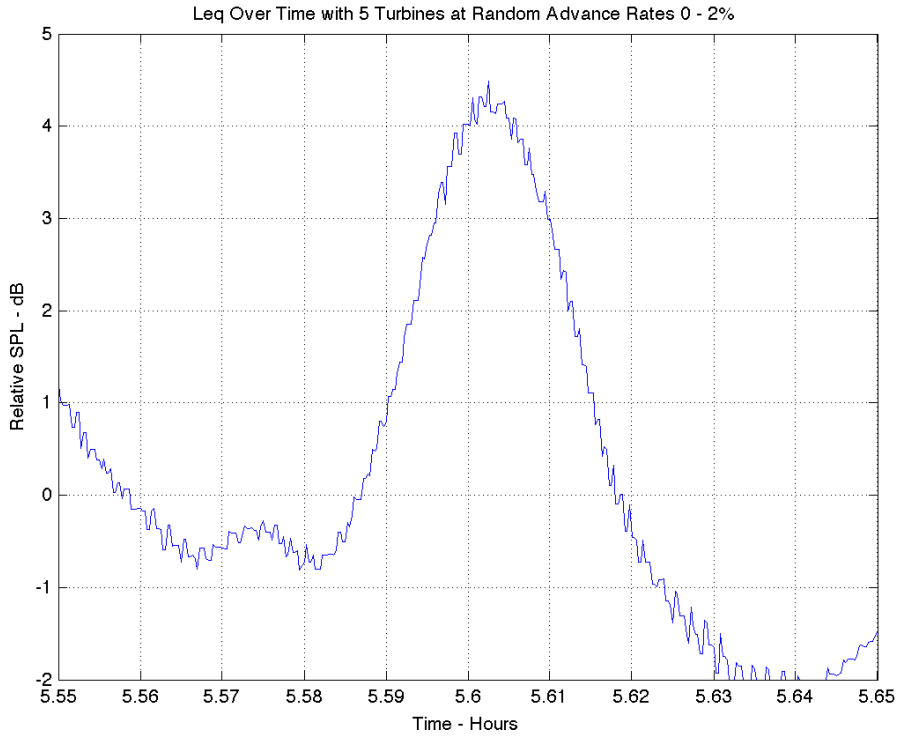

Figure 24. Expanded display of maximum noise event from Figure 22

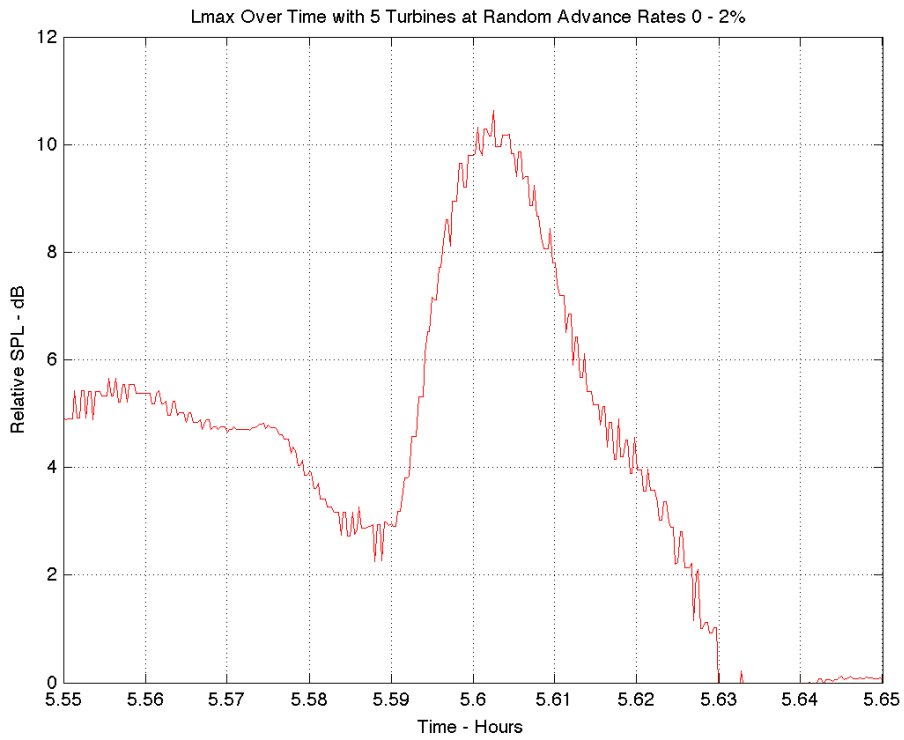

Figure 25. Expanded display of maximum noise event from Figure 23

Conclusions

The fundamental conclusion from this analysis is that one needs to be aware of coherent properties of the distinctive elements of wind turbine noise. Coherent addition of tones can result in increased uncertainty in measurements of emissions tonality and un-masking at noise-sensitive receptors. Temporary synchronization of low frequency impulses could cause overrun of non-linear structural response or subjective sensation thresholds.

For modest sized turbine arrays, the probability for worst-case combinations of tone phases or rotor blade thump timing is extremely low, but probability of increases in the range 3-5 dB is on the order 1-10%. The rarity poses enforcement and diagnosis problems; a resident awakened by a minute of window rattling might contact a complaint “hot line” and the synchronization that caused the rattling may never occur while the problem is investigated.

Mitigation Strategies

IEC standard 61400-11 appears to address the coherent addition issue by requiring identification of tones that have audibility greater than -3 dB. What is not addressed in the potential effect of multiple or distributed tonal sources with equal or nearly equal frequency on the measurement spectra. Equal-frequency sources that are not consistent in relative phase will combine to produce a different directivity pattern every time they are activated. Multiple sources that are phase-linked will have quasi-consistent directivity, but for source spacing greater than a small fraction of the wavelength, the directivity will be too irregular to assess reliable from a single measurement position. Aside from the obvious approach of minimizing tone production by individual turbine elements, minimizing the number of elements that produce the equal tone frequencies would reduce measured tone emission uncertainty.

In the author’s opinion, the current $\pm$ 20% tolerance on measurement distance exacerbates the problem. Measuring on a grid surrounding the IEC reference position would improve the confidence in turbine tonality ratings.

Rotor blade pulsation may be an unavoidable consequence of large turbine size, wind profiles and structural requirements. However, also as a consequence of large turbine size, noise sensitive receptors are generally only within the influence of a relatively small number. Conversely, location of turbines in relatively sparsely populated areas means that a turbine sub-array may only influence a small number of receptors.

A proposed strategy for pulsation mitigation is

1. Incorporate pulsation characterization into IEC 61400-11.
2. Determine, through analysis of turbine and receptor coordinates, the potential pulsation levels at the receptors having a generally accepted probability
3. For receptor locations where the potential pulsation levels exceed criteria, interlink the turbine controllers and program them so that blade position combinations that cause excessive pulsation amplitudes in the specific directions are avoided.

References

1. Kelley, N.D.: A Proposed Metric for Assessing Potential of Community Annoyance from Wind Turbine Low-Frequency Noise Emissions: Windpower ’87 Conference and Exposition, November, 1987.
2. Hubbard, H and Shepherd, K: Wind Turbine Acoustics: NASA Technical Paper 3057, December, 1990.
3. Procedure for Measurement of Acoustic Emissions from Wind Turbine Generator Systems, Volume 2: American Wind Energy Association Acoustic Standards Committee, October, 1992
4. Sutherland, L and Brown, R: Measurement and Evaluation of Environmental Noise from Wind Energy Conversion Systems in Alameda and Riverside Counties. Wyle Research Report WR 88-19, Wyle Research, El Segundo, California. October, 1988. [Includes a very inclusive bibliography]
5. Walker, B.E.: Signal Processing for Windmill Noise Measurement: JASA 80S1:S29, December, 1986.
6. Miles, Jeffrey Hilton: Aligned and Unaligned Coherence: A New Diagnostic Tool. NASA/TM—2006-214112 (AIAA-2006-0010), 2006.
7. International Standard 61400-11 Wind Turbine Generator Systems: Acoustic Noise Measurement Techniques, Edition 2.1, 2006.
8. Oerlemans, S: Detection of aeroacoustic sound sources on aircraft and wind turbines: Thesis University of Twente, Enschede: September, 2009
9. Low Frequency Noise from Large Wind Turbines: EFP-06 Project Report: Delta, November, 2010
10. Proceedings of WTN2007 and WTN2009